Molecular Crystals and Liquid Crystals Science and Technology. Section A. Molecular Crystals and Liquid Crystals

Publication details, including instructions for authors and subscription information:
http://www.tandfonline.com/loi/gmcl19

Control of Molecular and Supramolecular Architecture of Polymers, polymersystems and Nanocomposites

Gerhard Wegnerc [a]

[a] Max-Planck-Institut für Polymerforschung, Postfach 31 48, 6500, Mainz, Germany

Version of record first published: 05 Dec 2006.

To cite this article: Gerhard Wegnerc (1993): Control of Molecular and Supramolecular Architecture of Polymers, polymersystems and Nanocomposites, Molecular Crystals and Liquid Crystals Science and Technology. Section A. Molecular Crystals and Liquid Crystals, 235:1, 1-34

To link to this article: http://dx.doi.org/10.1080/10587259308055176

Mol. Cryst. Liq. Cryst. 1993, Vol. 235, pp. 1–34
Reprints available directly from the publisher
Photocopying permitted by license only

Printed in the United States of America

CONTROL OF MOLECULAR AND SUPRAMOLECULAR ARCHITECTURE OF POLYMERS, POLYMERSYSTEMS AND NANOCOMPOSITES

GERHARD WEGNER
Max-Planck-Institut für Polymerforschung, Postfach 31 48,
6500 Mainz/Germany

Abstract This contribution describes the rational step-by-step construction of molecular solids useful for the field of molecular electronics. Chain stiffness as a structural principle leads to the design of the macromolecules which already in a molecularly disperse state show effects expected for 1-dimensional solids. Phthalocyaninatopoly (siloxane)s are described as a typical example. The optical spectra of these polymers are explained based on the theory of 1 - D excitonic interactions. Such polymers can be subjected to the Langmuir-Blodgett-technique. Monolayers of the rod-like macromolecules at the air-water interface are transferred to solid substrates with concurrent orientation of the rod-axes into the dipping direction. Anisotropic multilayers are obtained in which the rods are stacked regularly in layers. When rods of different chemical composition are used a series of different architectures can be achieved, e.g. nanocomposites composed of layers alternating in chemical structure and direction of the rods. Such systems show interesting optical, electrochemical and electrical properties when properly composed. Furthermore, guest molecules can be placed ("doped") into the matrix of the side-chains in which the rod-backbones are embedded. Thus, when ionophores are chosen as guests, ion-sensitive membranes can be achieved. Their application to build ion sensitive FET-devices is described.

HAIRY ROD MOLECULES: BASIC CONCEPTS

A popular method to construct supramolecular architectures consists in the application of the LB-method to amphiphilic molecules spread as mono-molecular films at the air-water-interface of a Langmuir through. [1-3] Recently, a new type of molecular design was introduced in which the formation of a layered assembly at the air-water-interface depends on the form-anisotropic

shape of non-amphiphilic entities. Rod-like macromolecules decorated with short and flexible hydrocarbon side-chains as to provide the rods with a molecularly defined skin of solvent segments have been designed and tested[4-13]. They are spread from conventional solvents to the LB-through and compressed to a two-dimensional nematic liquid-crystal phase. The latter is transferred to solid planar substrates. A single layer is transferred by each dipping and undipping. Orientation of the rods is observed to occur in the dipping direction, so that anisotropic multilayers are obtained. The multilayers behave as solids with regard to their mechanical properties but as liquids with regard to their optical and other properties[14-17]. In fact, the architecture of these layers is best described as molecularly defined rods embedded in a continuous matrix of the liquid-like side-chain-segments. This unsual architecture belongs to the category of 'molecular composites'. It opens a number of possibilities to construct even more complex but still molecularly and topologically well defined supramolecular architectures.

The design principle of hairy-rod type polymers is lined out in very general terms by Fig. 1a. The backbone consists of any type of macromolecular structure with large persistence length as to allow for an overall form-anisotropic shape. The backbone of preferably cylindrical symmetry is modified by attaching short (typically $C_6 - C_{18}$) side chains as to provide a solvent skin which contributes the necessary conformational degrees of freedom to ensure solubility and tractability of the rigid rod macromolecules. Frequently long and short side chains are mixed within the same macromolecule in order to optimize the liquid like character of the skin. The architecture and type of interactions which characterize the layered structures is shown by Fig. 1b. The side chain moieties give rise to a continuous matrix in which the backbones are embedded as reinforcing elements. A packing of overall cylindrical hexagonal type is generally observed when the materials have been brought into equilibrium after a short annealing step. The lattice parameter of the hexagonal unit cell depends on the thickness of the solvent skin surrounding each individual rod and is thus open to molecular design. It is typically between 0.5 and 2 nm in the examples described further on. The process of spreading and assembly of these molecules is illustrated by Fig. 2.

The chemical design of the hairy-rods is open to variations. Phthalocyaninato(polysiloxane)s (c. f. Fig. 4) substituted with alkoxy chains at the

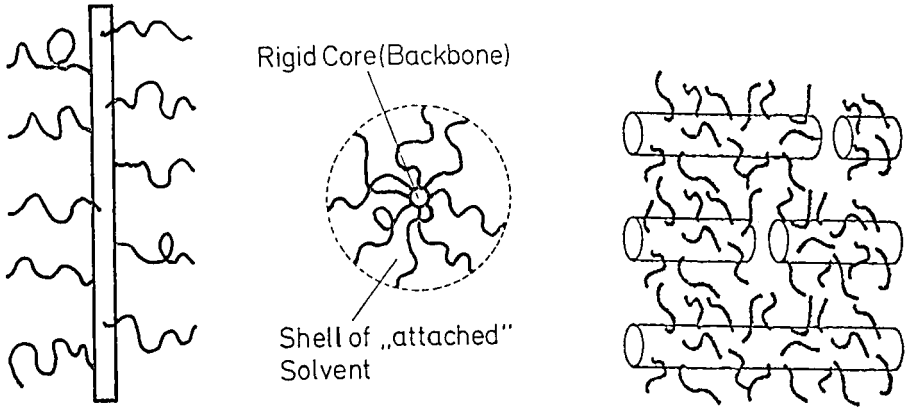

FIGURE 1 Hairy-rod macromolecule; the concept (left) and assembly form (right)

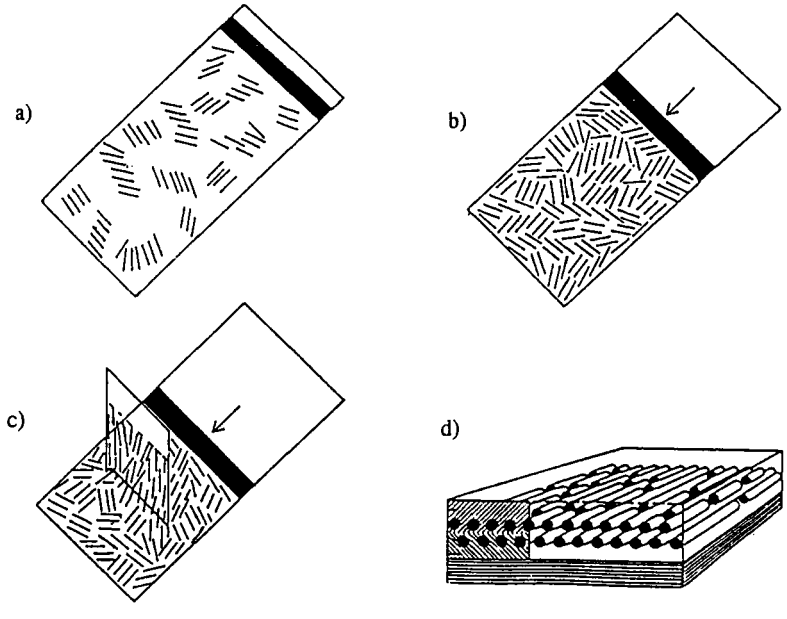

FIGURE 2 Assembly process of multilayers of hairy-rod macromolecules by the LB-technique[4]; a) polymer is spread to the air-water interface and b) compressed into a liquid crystal monolayer; c) Transfer occurs by dipping a substrate through the monolayer and d) flow induced orientation gives highly regular multilayers.

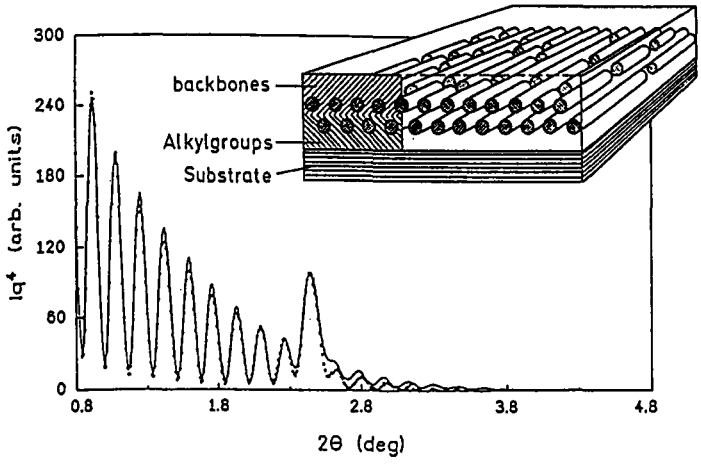

FIGURE 3 X-ray reflection pattern of a 28 layer assembly of a copoly(glutamate); only 2 layers are shown.

TABLE I PcPS-derivatives conforming to the hairy-rod concept;

Type	Nr.	R_1	R_2	R_3
PcPS ($C_1C_{8//}$)*	8	OCH_3	$O(CH_2)_6CH{=}CH_2$	H
PcPS ($C_{10//}C_{10//}$)	9	$O(CH_2)_8CH{=}CH_2$	$O(CH_2)_8CH{=}CH_2$	H
PcPS (C_1C_8)*	10	OCH_3	OC_8H_{17}	H
PcPS D_8(C_6C_6)	11	OC_6H_{13}	OC_6H_{13}	H
PcPS D_8($C_{10}C_{10}$)	12	$OC_{10}H_{21}$	$OC_{10}H_{21}$	^2H (D)
PcPS D_8($C_{18}C_{18}$)	13	$OC_{18}H_{37}$	$OC_{18}H_{37}$	^2H (D)
PcPS($C_{10}OHC_{10}OH$)	14	$OC_{10}H_{20}OH$	$OC_{10}H_{20}OH$	H
* Copolymer composed of positional isomeric repeat units.				

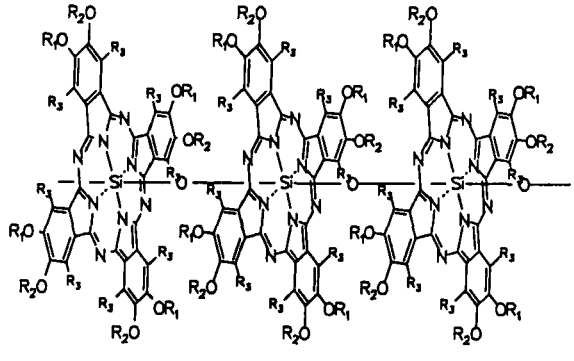

FIGURE 4 Three repeat units of PcPS (for R_1-R_4 see Table I)

perimeter of the phthalocyanine moiety serve as the prototype example and give high quality LB-layers[7-9]. A further example is provided by co-poly(glutamate)s in their helical conformation. Copolymers in which short and long side chains are mixed randomly proved to be execellent for LB-assembly[6,10,11,17]. The helical conformation of these macromolecules provides for the rod like character. Cellulose is an intrinsically worm-like macromolecule. If functionalized with alkoxy groups, it provided further examples of hairy-rods[12,18,19]. Finally, poly(silane)s conform with the ideas of a rod-like behaviour, if the side-groups R are designed to introduce sterical hindrance with regard to bending and to provide flexible groups directed to the outside of the molecule at the same time[13]. Similarly, poly-p-phenylenes substituted properly with sterically assuming, that is branched, alkoxy side chains will conform to this design principle[20].

The quality, perfection and stability of the layered assemblies and details of their internal architecture can be analyzed by a combination of different methods such as X-ray diffraction, spectroscopic (IR, UV-Vis, Raman) techniques, wave-guide spectroscopies etc[11,18,20]. As an example Figure 3 shows the small-angle-X-ray diffraction obtained from an assembly of 28 poly(glutamate) layers on a silicon wafer. The insert in Fig. 3 represents a molecular picture of the assembly with only two of the 28 layers drawn.

The degree of orientation of the rods within a layered assembly can be characterized by optical spectroscopy, birefringence or diffraction data. The order parameter depends on the flow conditions during the build-up of the assembly[22]. It is improved by annealing afterwards. Alignement of the stems parallel to the dipping direction in the course of the LB-process is only generated, if convergent flow conditions are provided together with extentional flow of the monolayer toward the substrate during the transfer process.[22,23] Therefore, the orientation of the molecular axes characterized by an order parameter S and in consequence the anisotropic properties of the layered assemblies like index of refraction, dichroic absorption, elastic moduli, conductivity etc. are largely controlled by the "deformation induced" orientation of the monolayer at the air-water-interface.[23]

PHTHALOCYANINATOPOLY(SILOXANE)S (PCPS)

Since the first report on the excellent LB-properties of the non-amphiphilic PcPS[7] (c. f. Fig. 4) many aspects of this type of polymer have been investigated.[8,9,23-26] PcPS as synthesized by Caseri and Sauer[24] have a large degree of polymerization. A representative list of derivatives differing in type, polarity and functionality of the side-groups at the perimeter of the Pc ring is compiled in Table 1. Most experiments have been carried out with polymer 10 which is the prototype material. It is generally called PcPS in the further text, if not stated otherwise.

The close cofacial packing of the monomer units along the polysiloxane chain, which is shown in Fig. 4, leads to a rather strong interaction between repeat units and results in a Si-O-Si bond angle of 180°. Furthermore, the repeat distance of 3.33 Å is considerably smaller than the van der Waals distance between planar aromatic hydrocarbons in molecular crystals, which is usually in the range of 3.4 - 3.6 Å. Due to this strong steric interaction, a bending of the polymer main-chain is not possible and indeed has not been observed. The rod-like character has been verified by detailed studies of the solution properties of PcPS by X-ray small angle scattering techniques.[9]

The packing of the Pc chromophores gives rise to very significant features when the molecule is photoexcited. The absorption spectrum of PcPS as well as that of the corresponding monomer is shown in Fig. 5. The monomer exhibits two regions of absorption: the B or Soret band at 340 and 358 nm and the Q band located at 680 nm with vibronic side bands at 651 and 612 nm. The Q-band of the polymer is shifted to 576 nm. Both bands arise from allowed $\pi^* \leftarrow \pi$ transitions with the transition dipole moments lying in the ring plane. Because of the nearly D_{4h} symmetry, the lowest unoccupied molecular orbital (LUMO) is doubly degenerate.

The cofacial arrangement in the polymer leads to a strong mutual interaction of the chromophores which results in a considerable blue shift of the maximum and a broadening of the Q band. These spectral changes can be explained with the theory of molecular excitons as given by Kasha.[27]

We consider the following dimer model (Fig. 6): two planar, cofacial chromophores are separated by a distance r_{12}. The transition dipole moments are lying in the molecular planes defining a torsion angle α when viewed along r_{12}. This, in the limit of strong coupling, leads to the energy level

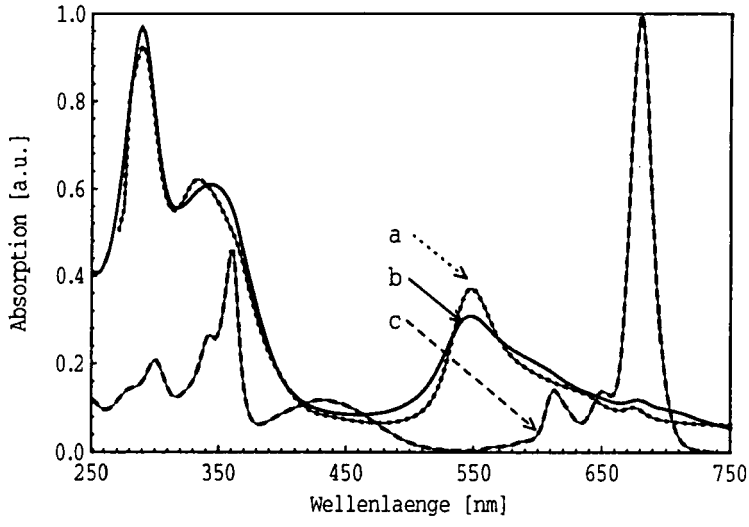

FIGURE 5 UV-Vis-spectra of PcPS **8** in a) toluene and b) $CHCl_3$; c) the spectrum of the corresponding monomer in $CHCl_3$

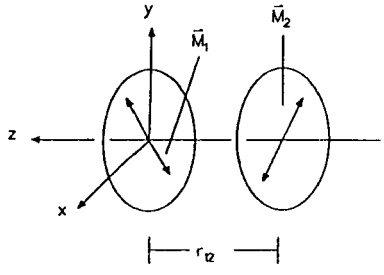

FIGURE 6

Exciton band scheme of a molecular dimer with parallel transition dipole moments (for explanation of symbols see text)

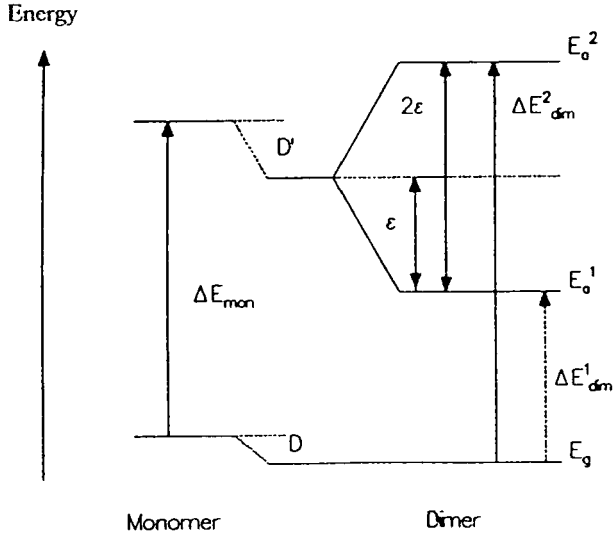

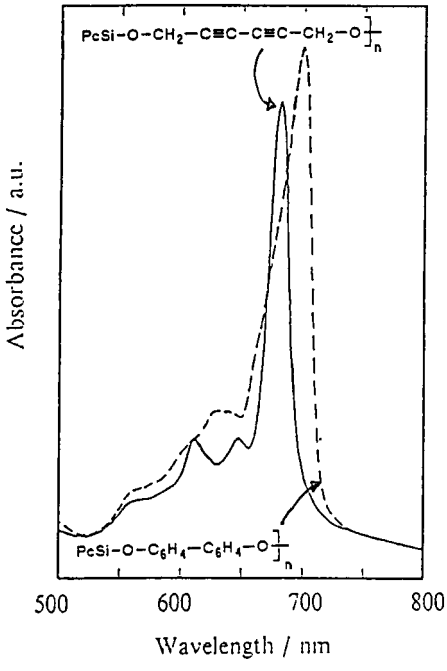

FIGURE 7

UV-Vis-spectra of PcPS with rigid spacer units between the Pc-rings

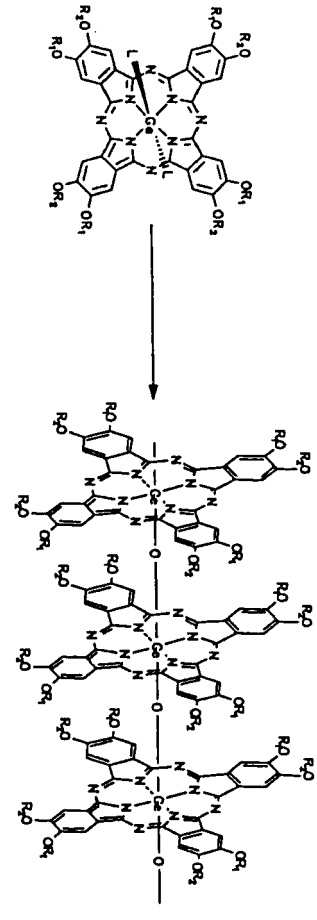

FIGURE 8 Synthesis of PcPGe

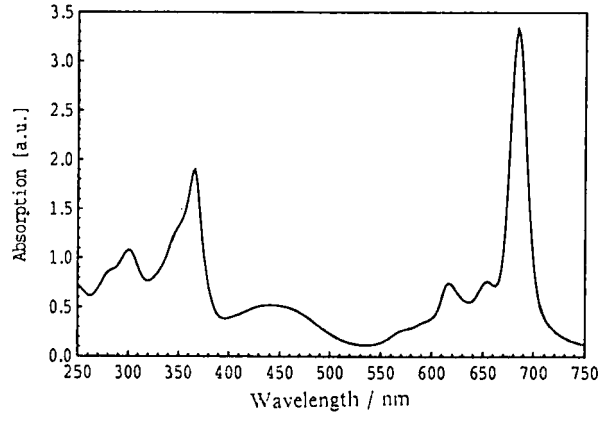

FIGURE 9 UV-Vis-spectrum of PcPGe

diagram shown in Fig. 6. The main result of the interaction is the splitting of the excited state. Using the point dipole approximation the exciton splittling energy is given by[28]

$$2\varepsilon = -(E_a^2 - E_a^1) = -2\frac{\bar{M}^2}{r_{12}^3}\cos\alpha \qquad (1)$$

M is the transition dipole moment which is related to the experimental value of the oscillator strength f. Although eq. (1) suggests that the exciton splitting 2ε can be determined experimentally, only the higher energy transition ΔE^2_{mon} of the dimer is allowed by selection rules when $\alpha = 0$. In the case of $\alpha > 0$ also the lower energy transition is weakly allowed, but in general only one level of the splitted exciton band can be observed experimentally as a peak in the spectrum.

Another possibility to determine 2ε and also α arises from the magnitude of the band shift.[25] The dimer transition energy ΔE^2_{dim} is given by[27] (see Fig. 6)

$$2\varepsilon = 2\left[-(\Delta E^2_{dim} - \Delta E_{mon}) + \Delta D\right] \qquad (2)$$

The generalization of this model to the case of a polymer with the degree of polymerization N results in an exciton splitting energy of

$$2\varepsilon = -4\left[\frac{N-1}{N}\frac{|\bar{M}^2|}{r^3}\cos\alpha\right] \qquad (3)$$

where r is the repeat distance in chain-direction. Combination of eq. 1 and 3 under the assumption that the numerical value of $\Delta D = -615\ cm^{-1}$ and r = 3.33 Å gives a value of the exciton splitting $2\varepsilon = -8448 \pm 112\ cm^{-1}$.

Furthermore a value of $\alpha = 73°$ is evaluated[25] which, because of the fourfold symmetry of the Pc chromophore corresponds to a geometrical rotation of adjacent rings around the common axis by about 17°.

A non-vanishing value of α due to rotational defects along the chain would lead to a weakly allowed lower energy transition. Therefore, one expects a slowly decaying intensity of the Q-band because of a sequence distribution of stacks having the correct torsional angle separated from each other by units with the "wrong" rotation angle. Furthermore, endgroups would

also act as defects and would give rise to finite intensity of the lower energy transition.

These results give valuable guidelines on what has to be done if a reduction of 2ε is wanted in order to tailor macromolecules with their optical properties ranging between the two extreme cases of monomer and polymer. The torsion angle α is very difficult to control, since it is determined by packing forces between phthalocyanine units along the polymer chain. The most obvious possibility is to increase r between adjacent Pc units. The introduction of spacers between the phthalocyanine units changes this separation on a large scale so tat we have a possibility to achieve monomer-like spectra as shown in Fig. 7. The nature and the length of these spacers can be varied to a great extent[29]. Besides the fact that the molecular exciton model is not applicable any longer in this case of very weak coupling, the mere fact that the exciton bandwidth 2ε depends on the inverse cube of the inter-chromophore separation explains why polymers with dioxybiphenyl- or hexadiindioxy-spacers between the Si-atoms of adjacent Pc rings along the chain where r is of the order of magnitude of 10 Å reproduce the optical spectrum of the isolated phthalocyanine. This design of spectral features and control of the excited state interactions is quite relevant for the area of nonlinear optics, here specifically for third-harmonic generation[29].

Phthalocyaninatopoly(germanoxane)s (PcPGe)

Soluble polymers equivalent to PcPS but containing Germanium as the bridging unit instead of silicon have been synthesized by S. Schwiegk[30]. The synthesis follows the principles developed for PcPS and is described by Fig. 8. The optical spectrum of the monomer 15 is shown in Fig. 9. The polymer spectrum resembles exactly the one observed for PcPS with the difference that, because of the larger spacing between the rings caused by the Ge-atom, the polymer Q band is less blue shifted. A polymer of degree of polymerization N = 15 showed the Q-band maximum at λ = 575 nm. The PcPGe polymers behave essentially the same as the PcPS polymers in the LB process and high quality multilayers have been obtained.[30]

STRUCTURE AND DYNAMICS OF THE LB-ASSEMBLIES

Phthalocyaninatopolysiloxanes (PcPS) (c. f. Fig. 4) substituted with methoxy- and alkoxy-side-groups at the perimeter of the metallomacrocycle were the first examples of hairy-rod molecules to be tested for the LB-technique[7,8]. Excellent spreading and transfer behavior is observed when side-groups of different chain-length and size are combined in the same molecule. PcPS derivatives with all side-chains of the same kind generally show the phenomena of side-chain crystallization which prevents the formation of a liquid-crystalline surface state at the air-water-interface; the transfer to solid substrates is then uncomplete and multilayers of acceptable quality cannot be obtained.

The rod-length (degree of polymerization) does not play an important role in the LB-process within the limits available by the synthetic methods. End-group-association in the course of the assembly may lead to a longer then the chemically defined length of the cylindrical building units. The force-area-diagrams characterizing the surface state of the molecules[8] are strongly temperature dependent but rather independent on pH or ionic strength of the water subphase. Transfer is typically achieved at constant surface pressure of ca. 20 mNm^{-1} and high transfer speeds (~ 1 - 2 cm min^{-1})

Spectroscopic (IR, UV, Vis), optical (birefringence) or diffraction techniques are useful[5,17,31] to characterize the order parameter of the alignement of the rod axes. They are generally oriented preferentially parallel to the transfer direction of the monomolecular film onto the substrate (c. f. Fig. 2). The linear dichroism of LB-films of PcPS is shown in Fig. 10. The second moment of the 2-dimensional orientation distribution of the rod axes can be derived from such spectral information[23]. Higher moments can be obtained from the anisotropy of the non-linear optical susceptibility $\chi^{(3)}$ as was shown by Neher et al.[32] X-ray reflection measurements near grazing incidence (c. f. Fig. 3) do not only provide information on the integral thickness of the layered assemblies and their internal periodicity but also about the roughness of the surface[18] The smoothness of the top surface is generally excellent and better than 0,6 - 0,8 nm in terms of a standard density fluctuaction about its mean value at the surface, that is much less then the diameter of an individual macromelecule which is about 2.0 nm for PcPS. The surface of a carefully prepared multilayer assembly of PcPS is completely featureless if

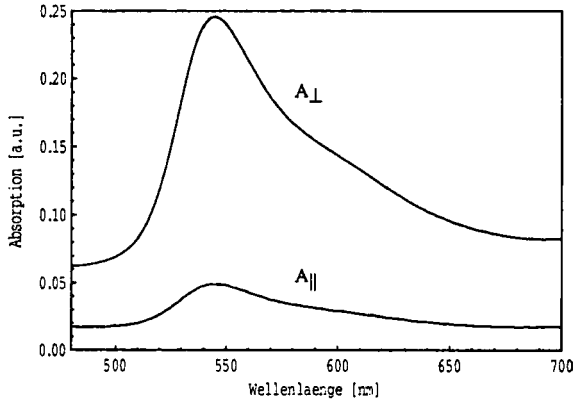

FIGURE 10

Polarized spectra of PcPS 10 (40 ML) on glass in the region of the Q-band

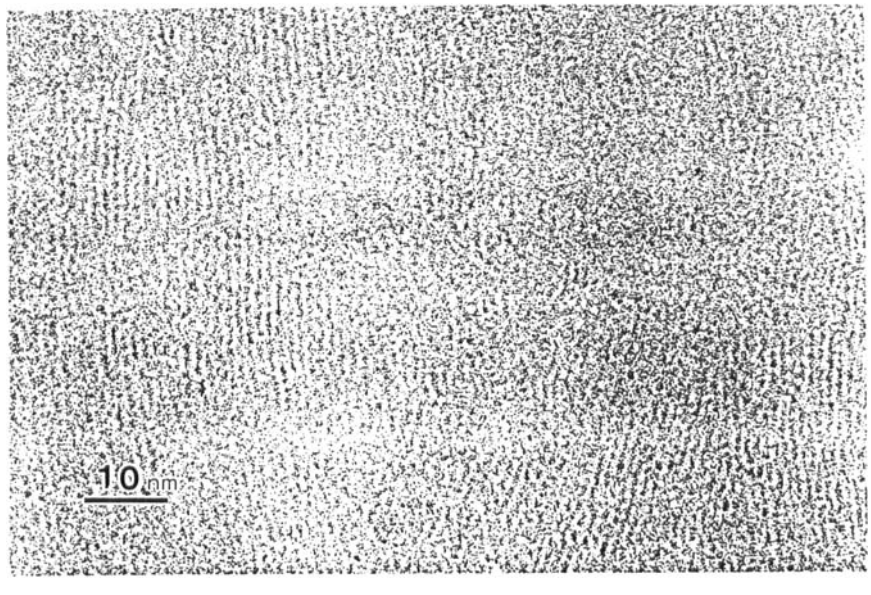

FIGURE 11 TEM image of a double layer of PcPS 8

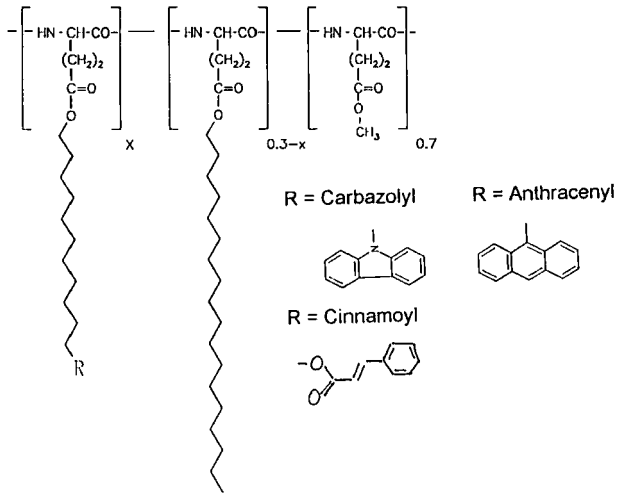

FIGURE 12 Structure of various functional copolyglutamates; $x \leq 0.1$ for cinnamoylderivative used for crosslinking, $x \leq 0.02$ for carbazolyl-/anthracenyl modified polymer.

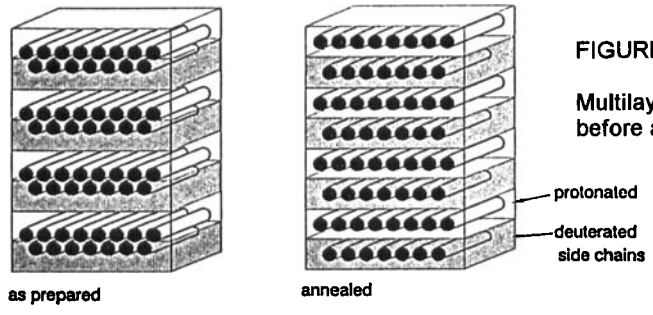

FIGURE 13

Multilayer assembly of PG before and after annealing

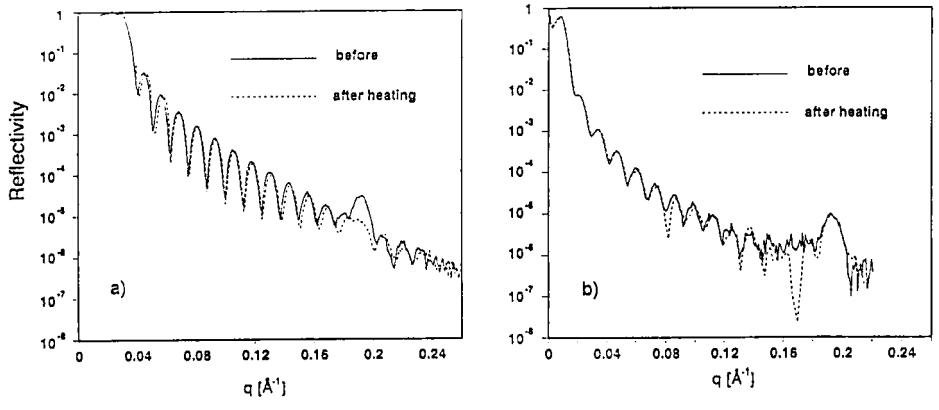

FIGURE 14 15 alternating double layers protonated/deuterated PG; a) X-ray reflexion b) neutron reflexion; annealing conditions: 4 h, 70° C

investigated by transmission or scanning type electron microscopes.[33] It is particularly important to note that no evidence for pinholes has been found so far even at a monolayer coverage if reasonably smooth substrates (e. g. window glass) had been used as the material to support the LB-film.

An excellent impression on the molecular architecture within the plane of the LB-assemblies can be gained by direct electron microscopic investigation in the case of PcPS[33,34] Here, PcPS 8 (c. f. Table 1) is used which contains double bonds in the side-chains. A double layer is transferred to an electron beam transparent substrate and is subsequently treted with O_sO_4 in order to enhance the contrast. TEM-pictures as the one shown in Fig. 11 will directly reveal the individual macromolecules aligned in the film plane to form a nematic like texture. Moreover, the individual rings stacked at a distance of 3.3 Å become visible. There is no evidence for defects other then the ones expected in nematic l. c. systems, specifically pinholes cannot be seen.

Copoly(glutamate)s as layered assemblies

The deposition behavior of polypetptides has been investigated extensively in the past[35-37] but was reported to be very poor. Therefore, in the past, these materials were not considered as useful in the production of multilayers of a reasonable degree of perfection. In our hands[6,10,11,14-18], high-quality multilayers of α-helix poly(alkylglutamate)s could be prepared when care was taken to prevent ordering phenomena induced by crystallization of the side-chain elements. This is achieved by selecting copolymers with an appropriate ratio of long and short alkyl side-chains. Detailed investigations were carried out for poly(methyl-co-octadecylglutamate) where the ratio of methyl/octadecyl of 3/10 to 6/10 was found to be the optimum. The copoly(glutamate) with a composition of 70 percent of all side-chains being methyl - the rest being long side-chains (octadecyl or functionalized alkylene chains) have become a "working horse" of the field. The chemical structure is indicated in Fig. 12, the structure of the assemblies in Fig. 3. Multilayer assemblies of this type are particularly interesting because of their optical[11,15] and mechanical[14,15] properties. The LB-assemblies are slightly birefringent (optically uniaxial) with the refractive index[11] parallel to the transfer direction (i. e. the helical axes) $n_{\parallel} = 1.500$ and $n_{\perp}$ (i. e. normal to the rod axes) = 1.486 at $\lambda = 633$ nm.

The alignment of the macromolecules with the helical axes along the dipping direction and the respective order parameter can be retrieved from dichroism in the infrared.[5] All vibrational bands related to the backbone (helical) segments are strongly polarized, the bands pertaining to side-group units are not. The 2-dimensional order parameter depends on the flow conditions during transfer of the monolayer[23] and may reach values of typically 0.8.

Thick layers can be built-up for optical measurements consisting of typically 1000 individual layers each of which is 1.75 nm thick. Analysis of the Brillouin spectra obtained from such layered assemblies by Stegeman, Knoll and coworkers[14,15] revealed that that we have an exemplary case of molecular composite formation. The Brillouin data allow for evaluation of the tensor elements of the elastic modulus of the layer assembly. Thus, C_{33} (in good approximation the Youngs modulus measured along the helical axis) has a value of 12.2 GPa and C_{13} has 4.2 GPa, to mention only two of the tensor elements.

Layer assemblies of copolyglutamates are thermally quite stable. The stability is limited by the occurence of irreversible helix-pleated sheat transition at temperatures above 150° C. The layers are stable below this temperature under open laboratory conditions over at least one year. Their optical quality and performance for optical waveguiding have been tested extensively.[11,16,17,21]

Translational diffusion and relaxation

The layered assemblies once prepared on top of a substrate have the texture of a frozen-in nematic liquid as far as the main chain director axis distribution is concerned. The order parameter S shows typically values of 0.35 to 0.4 in the as-prepared samples. It can be improved to values up to 0.8 in the course of a short annealing process at elevated temperatures (e. g. 1 hour at 70° C for copolyglutamates, 10 min at 130° C for PcPS[23].

Multilayer assemblies of PcPS are stable and do not undergo structural or chemical changes if annealed for several minutes at temperatures up to 270° C and may be exposed to ambient conditions over several hours at temperatures up to 150° C. This sets the limits of thermal stability for systems containing hairy-rods of this type.

A quantitative analysis[17,18,38] of the scattering data as shown in Fig. 3 reveals that double layers are formed initially upon transfer of the hairy-rods to the substrate which is usually made or selected to be hydrophobic. This structure relaxes to a hexagonal packing of the stems within the matrix of the side-chain-segments upon short annealing at moderate temperature (Fig. 13). A long range diffusion in terms of lateral or rotational diffusion of the rods is not observed. This is proven by experiments described by Fig. 14. It shows a) the SAXS pattern of an assembly consisting of 15 alternating double layers of the copoly(glutamate) shown in Fig. 12 and of the same copolymer with perdeuterated octadecyl side-chains and b) the corresponding small angle neutron scattering (SANS) pattern. The Bragg peak corresponding to the double layer periodicity in the SAXS pattern disappears upon annealing as a consequence of the structural relaxation and because the structure factor is to weak to provide intensity to the Bragg peak expected for the new hexagonal lattice. The Kiessig fringes remain unaffected indicating that the overall layer perfection and the surface smoothness do not change. The SANS pattern, however, clearly shows the Bragg peak caused by the superlattice periodicity of the alternating deuterated/non-deuterated molecular layers. It is not affected by the annealing procedure at all. Therefore, deuterated and non-deuterated molecules do not mix nor interdiffuse into each other. The results and consequences of this experiment are explained rather schematically by Fig. 13.

Further insights into the molecular dynamics and the related structural stability of these layered assemblies can be gained from photophysical studies on properly labeled molecules. Kuhn and coworkers[39] were the first to study energy transfer processes in LB-multilayer assemblies of classical amphiphiles doped with chromophores and showed that the Förster theory[40] can be applied to describe the distance dependent energy transfer by photostationary measurements. Yamamoto and coworkers[41] demonstrated that this technique may be used to characterize the structure of labeled amphiphilic polymers in LB-films.

In the present case where we deal with layers of rigid rods embedded in an matrix of side-chains, it is not only of interest to know about the periodicity of the rod axes but also about dynamical processes in the matrix. Therefore, two series of copolyglutamates were synthesized with carbazole and anthracene

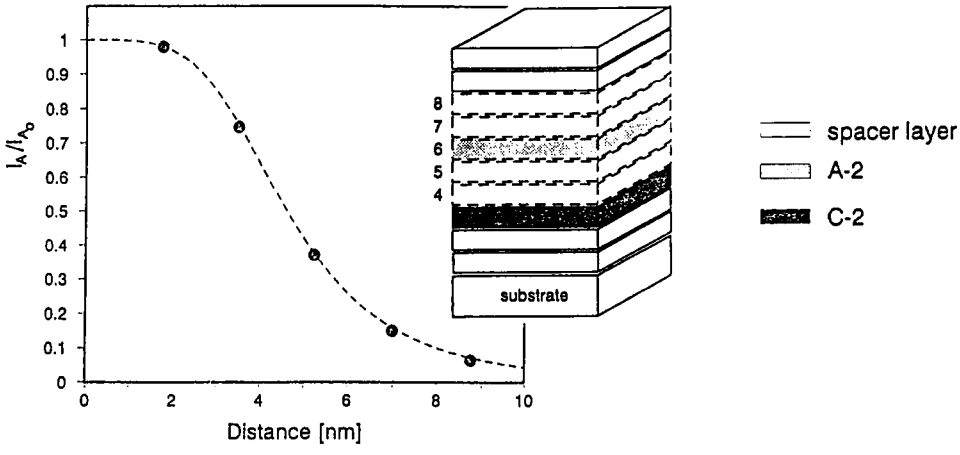

FIGURE 15 Multilayer assembly of PG modified by attached labels to study distance dependent energy transfer

FIGURE 16 Distance dependence of fluorescence yield (see text)

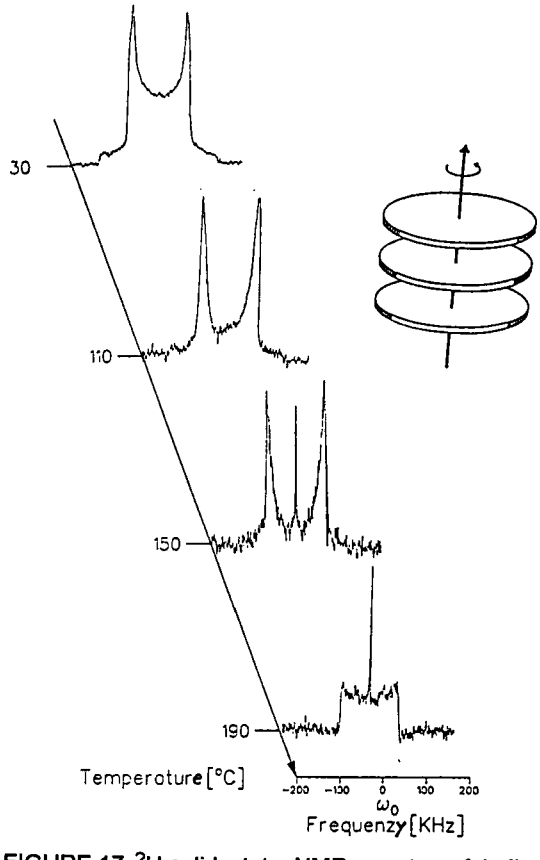

FIGURE 17 ^{2}H-solid state NMR spectra of bulk PcPS **11**, Table 1 at various temperatures and schematic view of the rotational jump motion.

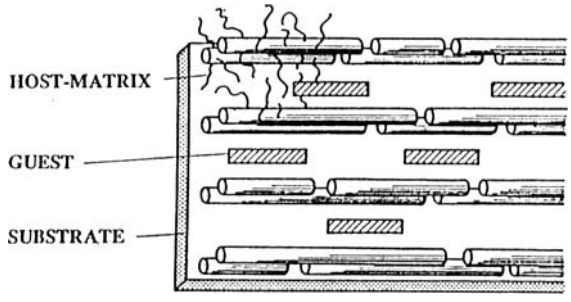

FIGURE 18 Host-guest system of form-anisotropic molecules embedded in an hairy-rod multilayer assembly.

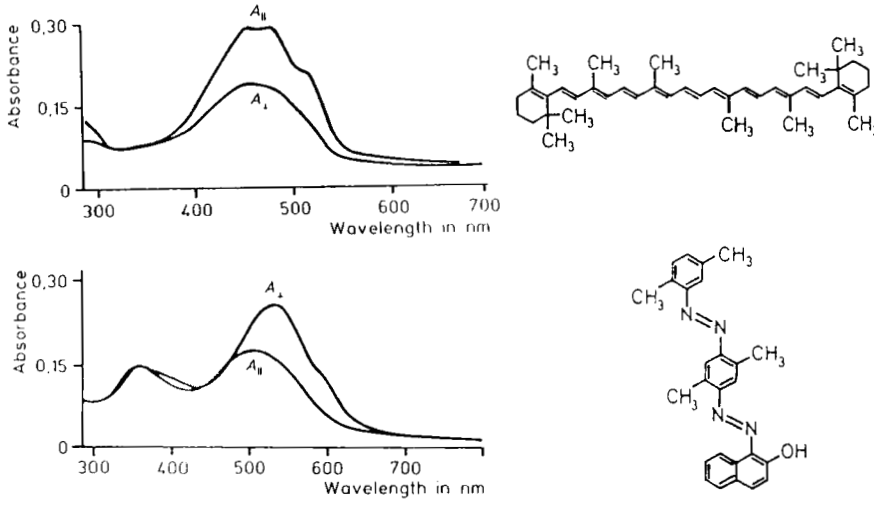

FIGURE 19 Dichroic spectra of β-carotene (above) and an azo-dye (below) in a copolyglutamate layered assembly[10]; $A_{\parallel}$ and $A_{\perp}$ refer to the rod director axis.

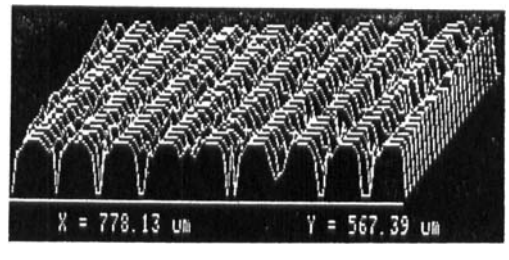

FIGURE 20 60 ML assembly of PcPS **8** processed into a stripe pattern by electron beam lithography.[22]

moieties covalently fixed to a small fraction of the side-chains. The structure of the polymers is shown in Fig. 13

The characteristic distance R_O (Förster-radius) at which half of the excitation energy is transferred from one to the other chromophore is ca. 2.9 nm[42]. Thus, the geometrical arrangement of the functionalized side-chains within the multilayer assemblies can be readily measured. The experimental set-up described by Fig. 15 was actually used[40]. The few attached chromophores (total molar fraction of chromophore labeled side-chains less than two percent) did not influence the LB-assembly process nor did they change the architecture of the assemblies. Multilayers gave a double layer periodicity of 3.5 nm by X-ray reflection and FTIR-spectra indicated the expected dichroism[5,6] and absence of other features but the α-helical conformation. The set of multilayer architectures consisted each time of ten monolayers where the third layer was made entirely of the carbazol-labeled one. The position of the layer containing the anthracenyl residues was varied by interdigitating 0 - 4 non-labeled copolyglutamate layers as spacers (c. f. Fig. 15)

The intensity of the fluorescence of the anthracenyl residues was measured as depending on the number of spacer layers, when the sample was irradiated at λ = 294 nm. The source for the anthracene fluorescence is the non radiative energy transfer from the photoexcited carbazole moieties. Thus, the relative intensity of the anthracene fluorescence I_A can be analyzed with respect to the distance dependence in the multilayer assemblies. According to Kuhn et al.[39] a relation between the energy transfer efficiency and the interlayer separation d in layered assemblies is expected as follows:

$$I_A = I_{A0} - d_0^{-4} \; (I_A d^4) \qquad (4)$$

I_{A0} is the fluorescence efficiency at complete energy transfer and d_0 is the Förster-radius corrected for a layered geometry. Fig. 16 shows the relative fluorescence intensity I_A/I_{A0} as a function of distance between the anthracene and the carbazol containing layer. The distance d was calculated with a monolayer thickness of 1.75 nm. The points can be fitted by a theoretical curve according to eq. 4 with d_0 = 4.63 nm. If we assume free-rotation of the chromophores in the matrix the Förster-radius R_0 may be calculated from $R_0 = (2d_0^4 / \pi \cdot \delta)^{-6}$. Here, δ is the area related density of the anthracene

chromophores. The concentration of anthracene labels is 0.7 percent; the area per repeat unit is 20 A^2 and, thus, the area per anthracene chromophore is 2860 A^2 which, in turn, provides a value of 4.5 nm for R_0. This is at variance with the tabulated value of 2.9 nm. The possible explanation is a higher apparent density of chromophores in the layer plane as a consequence of a local mobility of the labels within the alkane matrix in terms of a label diffusion. This ability of the chromophores to undergo rapid diffusion as much as it is allowed by the length of the chain by which it is attached to the polyglutamate backbone is also the reason for the fact that the distance dependence shown in Fig. 16 is fitted by a monolayer periodicity. d is obviously the average distance by which the donor and acceptor chromophores are separated from each other.

The assumption that the matrix of the side-chain behaves as an ordinary hydrocarbon liquid with regard to diffusion and selfdiffusion of dopant molecules whose hydrodynamic radii are smaller than the mesh-size defined by the periodic distance between the rods has been proven in separate experiments[44]. If such dopant molecules were co-spread with the layer forming polymer and transferred sequentially with non-doped layers, a very fast redistribution of the dopants took place within the time necessary to prepare the samples. Only samples without any periodicity of the dopants and containing the average concentration per layer were obtained.

Rotational Dynamics

The mobility of macromolecules can be characterized on a molecular scale making use of ^2H solid-state NMR spectroscopy. The geometry and frequency of motional processes can be examined even for segments of a macromolecule when selectively deuterated species are available[45]. Even ultraslow motions can be identified by 2D-exchange NMR spectroscopy as has been shown for low molecular weight discotic l.c. materials recently[46]. The rotation of stacks of molecules around the common columnar axis could be described as a "jump diffusion inside a three-fold potential"; this motion turned out to be directly linked to the dynamic glass transition.

In case of the PcPS type polymers the mesogenic phthalocyanine moieties are permanently linked together along the columnar axis. Therefore, rotations around this axis were expected to be active (Fig.17).

Since the hexagonal packing found for substituted PcPS is identical for bulk samples and for annealed LB-layers, the NMR investigations were carried out with the former[47] making use of the polymers 11 - 13 (Table 1) selectively deuterated at the ring position "R_3". Fig.17 shows temperature dependent one-dimensional spectra obtained for PcPS 11 with a solid-echo pulse sequence[48] with a time delay of 30 μs between the two pulses. 90° - pulse length was about 2.7 μs. PcPS 11 shows the typical behaviour of all such polymers where side-chain ordering does not exist. The room temperature spectra of the rigid Pake-type imply the absence of all rapid-rotational motion with amplitudes larger then ca. 5 degrees. The intensity of the broad spectrum decreases with increasing temperature, but only at T = 480 K motionally averaged spectra are obtained. These findings are consistent with an axial-rotation of the molecules around their long axis as it is typical for other discotic l.c. phases. The rotation-rates at 480 K are higher than 10^6 Hz. 2D exchange NMR spectra[47] observed at 340 K confirm that this motion exists already at this temperature albeit with a correlation time of only a few ms. This spectra could be simulated assuming a four fold jump including significant deviations from the ideal jump angles of 90° and 180° similar to what has been found in discotic triphenylene-based materials[46] The question whether the rotational motion involves whole macromolecules or monomer units only cannot be solved conclusively; it is, however, probable that the jump motion comprises packages of rings rather then individual repeat units. Otherwise one would expect sharp jump angles to be seen.

Hairy-rod multilayer assemblies as host matrix

The liquid like nature of the matrix in hairy-rod multilayer assemblies suggests experiments aimed toward their use as hosts for various types of guest molecules wich -by themselves- cannot be processed into mono- or multilayer form. In fact, a wide variety of oleophilic dyes can be cospread with copolyglutamates onto the air-water interface from a solvent in which the polymer assumes the helical conformation[10]. LB-assemblies are then built up as usual. Form-anisotropic dye molecules like β-carotene or azo-dyes are incorporated into the host matrix with a preferential orientation of their molecular long axis parallel to the director axis of the polypeptide chain.This is demonstrated by the schematic picture shown in Fig. 18 and by the dichroic spectra obtained for assemblies with β-carotene (Fig. 19a) and an azo-dye

(Fif. 19b) as guests. The origin of the directional effects is clearly related to te spatial restrictions of the space between adjacent-rods in the host matrix. The symmetry of the packing of the rods is not changed by the guest molecules; however, a certain degree off swelling up to 25 percent is observed at high loading of the matrix by guest molecules. The solubiltity of the matrix for guest molecules is limited and crystallization or phase separation sets in, when a critical space-filling concentration of the guests with regard to the available volume between the rods in the matrix is reached. The guest molecules are not fixed inside the matrix, however, but show rapid self-diffusion as in an ordinary liquid[44].

These findings have a number of very interesting consequences and implications. A few examples are:

- Sensitization of systems designed for crosslinking copolyglutamates containing functional cinnamoyl groups. These could be cospread with oleophilic triplet sensitizers and, thus, the photocrosslinking reaction could be carried out very efficiently irradiating into the sensitizer absorption band rather then using short UV-light-sources[17].
- Doping of copolyglutamate or PcPS layers on top of MOS-structures by ion-specific complexants in order to produce a selective ELBOS system (vide infra).
- Swelling of hairy-rod networks[50,51]
  Once a network is produced by crosslinking of the functionalized hairy-rods in multilayer assemblies they will readily incorporate low molecular weight solvent molecules and other molecules of swelling. The driving force for the incorporation is the osmotic pressure. Since different types of molecules can be incorporated simultaneously, an ultrathin layer reactor may be conceived provided the different type molecules would react with each other inside the host matrix.

Networks and Photoresist Patterns

Photocrosslinkable PcPS can be made incorporating double bonds into the side-chain moieties (c.f. 8 an 9 Table 1). The formation of patterns after irradiation through a mask and developing with a solvent for the non-crosslinked, that is unirradiated parts of the layered assemblies has been reported. Fig. 20 represents a stripe pattern produced by electron beam irradiation of PcPS 8 and development of the pattern in $CHCl_3$. The special

properties of PcPS do not allow to use them as wave guides in the visible. Copoly(glutamate)s, however, have excellent optical properties and it was, therefore, important to develop photocrosslinkable derivatives which conform to the LB-process. Terpolymers were developed[51] toward that purpose which contain cinnamoyl groups as photoreactive moieties (Fig. 13). Multilayers become totally crosslinked by irradiation and are insoluble in a solvent mixture ($EtOH/CHCl_3$) which would rapidly and completely dissolve the as prepared unirradiated assembly. The initial thickness of the multilayer decreases by ca. 5 percent after irradiation and solvent treatment and the periodicity (Bragg peak) changes from 3.5 to 3.3 nm. The surface roughness stays constant within the limits of error (0.57 nm). It is worth noting that the crosslinking reaction which is carried out at room temperature prevents the relaxation process to take place which has been described above (c.f. Fig. 13). Stripe wave guide patterns with excellent resolution and acceptable attenuation properties have been obtained along this line[17,52].

A very schematical description which is nevertheless correct in the important details of the networks based on hairy-rod components is shown by Fig. 21. Such novel network architectures have a number of implications for materials science (elasticity, strength, membrane separation processes).

Nanocomposites

Futher types of supramolecular architectures can be assembled using different types of hairy-rod macromolecules. Alternating layer structures are obtained by successive transfer of either of two compounds. An example, the superlattice composed of deuterated and non-deuterated species of the same molecular structure, has already been given (c.f. Fig. 13). A further example, an architecture of alternating double layers of PcPS and copoly(glutamate)[18] is shown in Fig. 22. Not only the chemical structure may alternate or follow any other design principle in terms of the layer-sequence but also the relative direction of the rods in each layer with regard to a frame of reference. The latter follows from the fact that the rod axis direction is related to the dipping direction. Therefore, if the substrate is rotated in-between subsequent dipping cycles the rotation angle will be identified as the angle between subsequent layers in the assembly. Similar structures as the one shown in Fig. 22 have been described using copolyglutamate and cellulose alkyl ethers[18]. The cellulose derivative contained double bonds in the side chain which could be

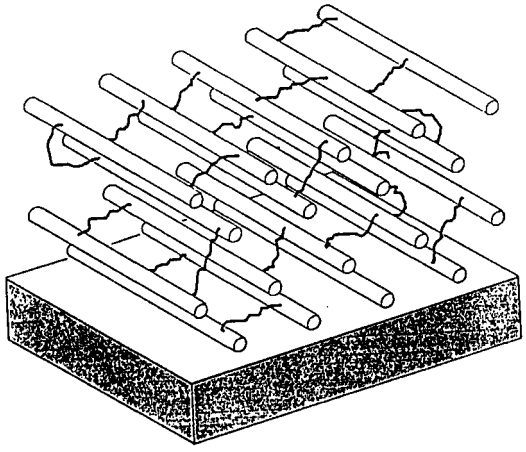

FIGURE 21

A network based on hairy-rod assemblies; the network chains are shown only, the residual non-crosslinked side-chains are left out.

FIGURE 22

Nanocomposite of alternating double layers of copolyglutamate and PcPS and corresponding diffractogram

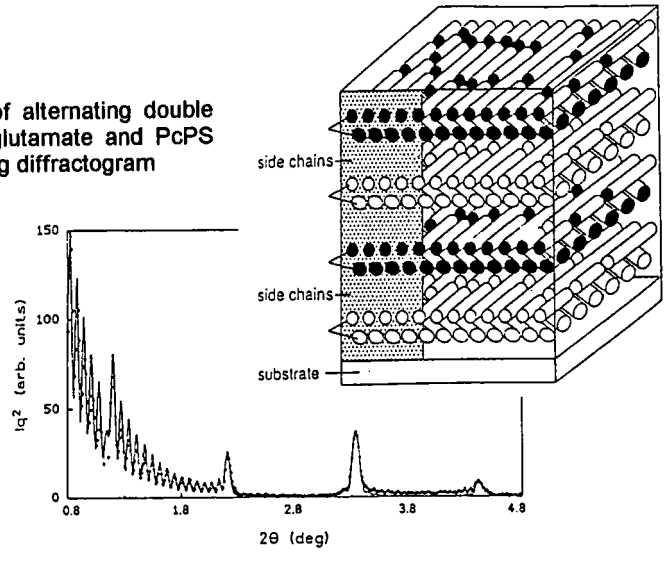

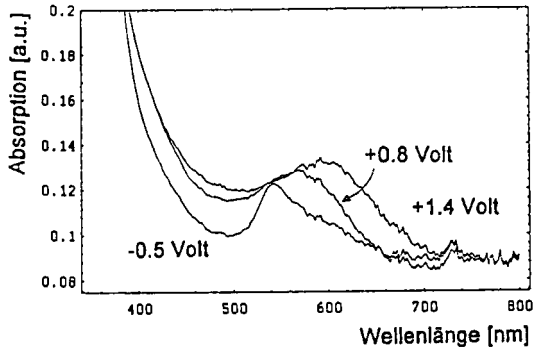

FIGURE 23

Spectro-electrochemistry of PcPS (see Text)

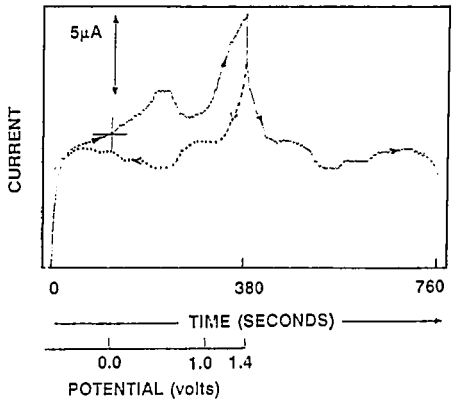

FIGURE 24

Cyclovoltammogram of PcPS (see Text)

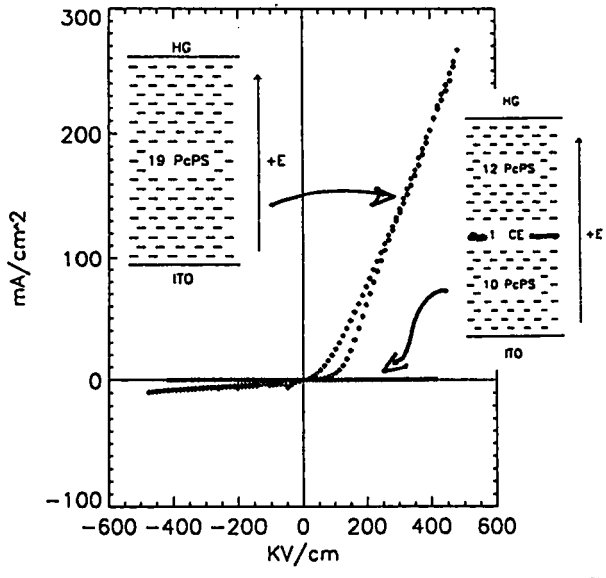

FIGURE 25 IV-curves of a multilayer assembly of PcPS (19 layers) and of an assembly of 22 layers of PcPS containing a single barrier layer of cellulose ether in the middle.

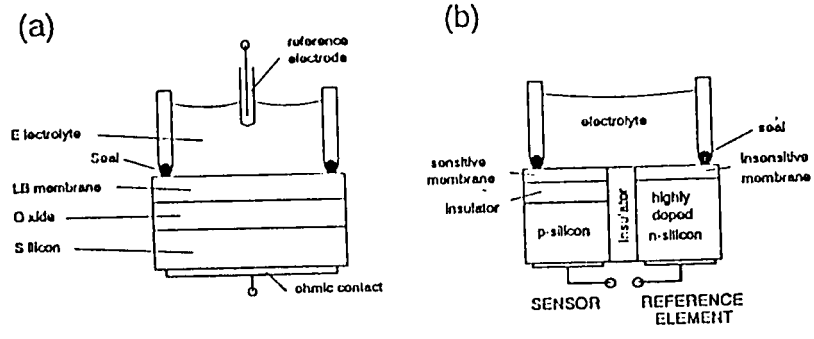

FIGURE 27 Cross-section of (a) an ELBOS (Electrolyte/LB-membrane/Oxide/-Silicon) structure and (b) of the capacitive sensor system (CSS).

reacted with OsO_4 without destroying the layered assemblies[18]. This is a further example for chemical reactions which can be carried out in the matrix of these molecular composites.The usefullness of such supramolecular structures in the design of functional systems, e.g. sensors, will be described below.

ELECTROCHEMICAL; ELECTRICAL AND SENSOR PROPERTIES

Electrochemical Oxidation of PcPS

Cofacially polymerized crystalline phthalocyanines predate the PcPS system and have been of interest because of the wide range of conductivities achievable as the degree of oxidation ("doping level") is varied[52]. Both chemical and electrochemical doping of the crystalline phthalocyanine polymers have been explored[52,53]. Doping with oxidants like I_2 gives a conductive phase (compound) with a ratio of counterion (e.g. I^-) to Pc monomer unit of ca. 0.33. The conductivities of all phthalocyanine based materials is similarly and very strongly affected by reaction with acceptors; in many cases oxygene is a sufficient strong acceptor to markedly influence the conductivity of phthalocyanines and derivatives if exposed to ambient conditions.

The exploitation of PcPS and related materials as electrochemically "addressable" molecular arrays and as the active interface in chemical sensors requires a quantitative description of the transport of both electrical and ionic charge through the layered assemblies. Patternable arrays (Fig. 20) can be formed utilizing photopolymerizable side chains attached to the redox active phthalocyanine moieties. Thus, highly differentiated electrochemically and in consequence electroactive structures on the microscopic scale can be envisaged. Some electrochemical data on PcPS have been reported previously[25]. In the following some recent experiments[54] will be discussed. Fig.23 and 24 show the voltammetry and spectroelectrochemistry of a preparation consisting of 22 monolayers (ML) of PcPS on an ITO electrode in CH_3CN, 0.1 M TBAP. The voltammetric data refer to a Ag/AgCl reference electrode. The oxidation wave seen in the region between 0.0 and +1.0 V is accompanied by a symmetric reduction wave on the return sweep. Systematic changes seen in the absorbance spectrum of the multilayer assembly during this oxidation/reduction process suggest in accordance with a coulometric

analysis that the same oxidation chemistry takes place in the range between 0.0 and +1.0 V despite the structure seen in the voltametric curve. At +1.0 V all the Pc rings in the polymer thin film have undergone a one-electron transfer of the type $Pc \rightarrow Pc^{+}$. The onset of a second, distinct process at potentials higher then +1.0V reflects the reaction $Pc^{+} \rightarrow Pc^{2+}$. Spectra were recorded throughout the oxidation/reduction sweeps; for the sake of clarity only a few spectra at selected potentials (degrees of electrochemical conversion) are shown in Fig. 24. The data indicate that a new spectral peak centered at 580 nm is formed upon oxidation which is linked to the increasing concentration of Pc^{+}. This species also causes substantial, albeit unstructured increase in absorptivity in the spectral region 420 - 470 nm. Positive of +0.9 V the absorbance at 648 nm rises sharply along with the oxidation current. All absorbance changes are reversed immediately scanning the potential negatively, suggesting conservation of PcPS chromophores.

Potential step experiments were used in conjunction with absorbance changes to estimate the effective diffusion rate of charge[55]. The apparent diffusion coefficient, D_{app}, actually a combined magnitude reflecting both electron exchange and ion-migration rate is obtained measuring the faradaic current flow in response to a potential step at known thickness of the film containing a fixed number of electroactive sites. For the 22 ML films described above and voltage steps of typically 0.6 V D_{app} were $1 - 2 \cdot 10^{-11} cm^2 sec^{-1}$ for the oxidation and $6 - 7 \cdot 10^{-11} cm^2 sec^{-1}$ for the reduction. These low values reflect the difficulty of ion migration in these very dense films of a polar nature as far as the matrix of hydrocarbon side chain is concerned in which the redox active Pc-stacks are embedded. It is also felt that the reason for the large width of the first oxidation wave relates to the difficulty to drive the counterions into this matrix which is necessary to reach electroneutrality.

At the other hand, this feature helps to render the redox cycle completely reversible. For instance, in CH_3CN/TBAP and on a gold electrode a 1 ML PcPS film could be reversibly cycled between the neutral and the first oxidized state for as many as 15.000 times without any sign of degradation. Only at potentials higher than +1.0 and prolonged exposure the films started to fail. PcPS films show superior performance as electrochemically blocking or mediating materials. Down to a coverage of 3 ML films of PcPS on Au-electrodes proved to be densely packed and impenetrable to solution species

such as hydroquinone, ferrocyanide and ferrocene (Fc). The facile oxidation of Fc to Fc^+ in water (ca. 10% $MeOH/H_2O, 0.1MHNO_3$) is blocked at its normal potential E°, when the Au-electrode was covered by 3 ML of PcPS, as is the oxidation of the added MeOH. Oxidation of Fc proceeded smoothly when the voltametric oxidation of the PcPS had taken place and the layered assembly had become conductive. On the backsweep the reduction of $PcPS^+$ back to PcPS blocked the reduction of Fc^+. Similar rectifications of electrochemical oxidation/reductions were observed for 1 - 100 millimolar concentrations of hydroquinone and ferrocyanide.

Conductivity Experiments

The possibilities offered by the assembly technique can be used to device a series of experiments which aim for an understanding of the molecular details of charge carrier motion. The current-voltage characteristics of assemblies of monolayers of PcPS between an ITO and a liquid mercury electrode shows an asymmetric transport behaviour. The layers stand quite large field strength up to $6 \cdot 10^5$ Vcm^{-1}. A short annealing step which improves the density of packing of the layers removes trapping centers. An excellent rectifying behaviour is now verified as expected for neutral, semiconducting PcPS which is a hole conductor.

The conductivity of a layered assembly depends strongly on the thickness, that is the number of ML in the assembly. This is a consequence of the tunneling controlled transport features.

Fig. 26 provides an overview of the measured conductivities as a function of the layer thickness. This plot integrates the conductivity data obtained from dc-measurements at small field strength as well as the frequency independent conductivities from ac-measurement. To a rough approximation the conductivity decreased exponentially with the number of monolayers $n \leq 40$. The gradient determined from Fig. 26 is about 0.08/monolayer so that the thickness dependence of the conductivity is approximated by $\sigma_{dc}(N) = \sigma_0 \exp(-0.18 * N)$ where N denotes the number of monolayers and σ_0 is given by $2.8\ 10^{-6}$ S/cm.

The conductivity behaviour changes dramatically when a **single monolayer of a cellulose** derivative as indicated in Figure 25 is inserted in the center of the layered assembly. The conductivity drops 3 - 4 orders of

magnitude and also the shape of the current-voltage characteristic changes substantially.

The monolayer of the cellulose derivatives serves as a tunneling barrier as envisaged by Kuhn and Mann[56]. Analysis[57] of I/V-data according to this ansatz gives a barrier width of s = 2.17 nm and barrier height of h = 2.2 eV in excellent agreement with expectations from the physical nature of the barrier.

Si-based Ion Sensors

Using the LB-films of hairy rods as a carrier of ionophores it is possible to manufacture highly sensitive and selective sensor-membranes[58,59,60]. As an example a Na^+-sensor is presented with a constant sensitivity of 53 m V/pNa for more than 61 days and a small baseline drift of only 1 mV/day. This is achieved by mixing a commercial Na^+-Ionophore with the LB-material before film deposition. Best results are obtained with a cross-linked cover-layer serving as a diffusion barrier for the ionophores but not for the ions to be detected.

The same LB-material as before but without ionophores can be used as a reference-membrane in a capacitive sensor-system (CSS). The special advantage of this sensor-system with sensor-and reference-membranes made of the same base-material is, that the influence of disturbing ions in the electrolyte is automatically compensated.

To obtain different sensitivites the gate of ISFET-devices[61] can be coated with inorganic or organic membranes. Most promising is the use of organic membranes with sensitive groups like ionophores. The ionophores can be covalently fixed or physically mixed to the carrier-membrane. So far the results with respect to longtime-stability, drift, and selectivity were not very satisfactory when conventional polymers or LB-films were used. The situation is changed with the hairy rod type materials.

A first success was the development of a pH-sensor with a stable LB-membrane made of PcPS[60] Another stable LB-material is poly(glutamate), which has very much lower pH-sensitivity, but no cross-sensitivities to various other ions[58,60]. Impedance spectroscopy (IS) and CV-measurements on combined layers (PG/PcPS and PcPS/PG) show, that the build-up of the electrical potential takes place inside the bulk of the LB-membranes. Obviously the ions are able to penetrate into the films. Therefore it seems to be possible to use such LB-membranes as a matrix for special ionophores.

The ionophores have to be well soluble in the sensitive membrane, but insoluble in water and in the material of the cover-layer. The cover-layer has to serve as a diffusion barrier for the ionophores but not for the ions to be detected. A Na^+-sensor was presented with a sensitive LB-membrane made of poly(glutamate) containing Na^+-Ionophores and a cover-layer of cross-linked PcPS.

In ELBOS (Electrolyte/LB-membrane/Oxide/Silicon)-systems a conventional Ag/AgCl reference-electrode was used (Fig. 27a).

To obtain a capacitive sensor-system (CSS) the sensor (Sensitive membrane/Oxide/Silicon) and a reference-element (PG/n^+-Si) were placed together in a flow-through cell. A cross-section of such a sensor system is shown in Fig. 27b.

Both, ELBOS- and the sensor-system are capacitors with capacities depending on the applied bias voltage.

The output signal is given by the shift of the CV-curves with the Na^+-activity of the electrolyte. The LB-membrane used in this example was made of poly(glutamate) containing 11% of the Na-Ionophore indicated and a cover-layer of pure poly(glutamate) (2 monolayers). The Na^+-sensitivity was linear in the range from pNa = 0 to pNa = 3 with53 mV/pNa.

Unfortunately, however, these systems show also a drift of the CV-curves depending on the time of storage in water. The drift always continued in the direction of positive voltages, and it was accompanied by a decrease of the Na^+-sensitivity in the range of lower pNa-values. The reason could be wash-out of the ionophores. To further improve the long-time stability special cover-layers of another material were used, which could be cross-linked by UV-light subsequent to the deposition. The results are shown in Fig. 28. This sample with a membrane made of poly(glutamate) with 11% Na-Ionophore (20 ML) and a cover-layer of PcPS (2 ML) during the first 14 days showed a drift of merely + 50mV, i.e. less than 4 mV/day. Up to the 61th day the drift even decreased to values of less than 1mV/day. During the whole time of observation the slope of the curves, that means the Na^+-sensitivity, remained constant.

The special advantage of the sensor-system presented by Fig. 27 is the compensation of cross-sensitivities.

This is possible when reference- and sensor-membranes are made of the same material and have the same sensitivity to disturbing ions in the

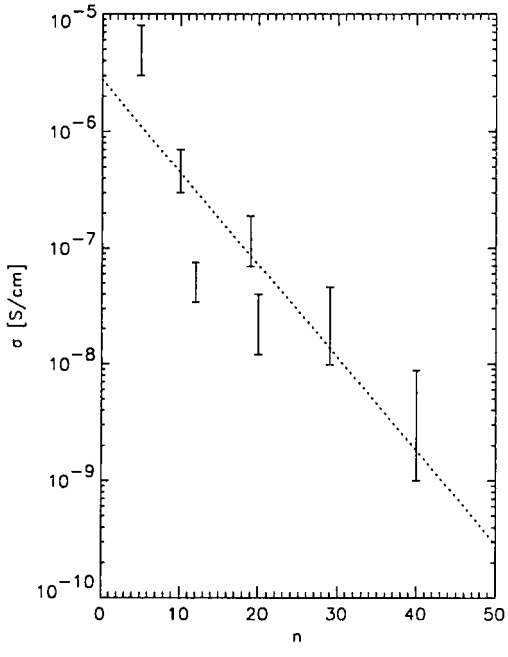

FIGURE 26 Conductivity of PcPS layered assemblies depending on the number n of layers

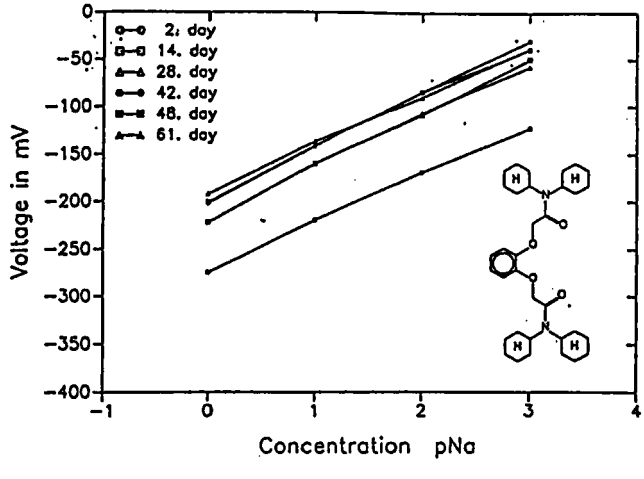

FIGURE 28 Long time study of ELBOS (see Text): drift of the sensitivity curve toward positive voltages, the sensitivity (slope) itself remaining constant.

electrolyte. In fact, the resulting sensitivity to these ions is very low. In a demonstrator set-up the Na^+-sensitive membrane was made of poly(glutamate) with 11% Na-Ionophore and a cover-layer of pure poly(glutamate). For the reference-membrane was used the same polymer without ionophores.

The sensitivity curve for Na^+ was linear in the range from pNa = 0 to pNa = 4 with 45 mV/pNa[25]. For a constant Na^+-activity of pNa = 3 the sensitivity of this Na^+-CSS to H^+-ions was less than 8 mV/pH in the range from pH = 3 to pH = 5 and from pH = 8 to pH = 11. Between pH = 5 and pH = 8 the pH-sensitivity was almost zero, and the Na^+-concentration could be measured independent of the pH-value.

Acknowledgement

This work was supported by the German minister of research and technology (BMFT) as a part of the project on "Ultrathin layers of Polymers as New Materials for Optics, Electronics and the Life Science". G.W. wants to thank the following coworkers and students for their contributions and intensive interaction:

PROF. N.R. ARMSTRONG, DR. T. ARNDT, DR. P. ALBOUY, DR. CH. BUBECK, DR. W. CASERI, DR. G. DUDA, DR. F. EMBS, E. FERENCZ, H. FISCHER, DR. W. HICKEL, DR. A. KALACHEV, DR. W. KNOLL, DR. L .LIESER, A. MATHY, DR. D. NEHER, DR. E. ORTHMANN, DR. A. RITCEY. DR. T. SAUER, M. SCHAUB, A. SCHMIDT, S. SCHWIEGK, M. SEUFFERT, DR. M. SCHULZE, T. VAHLENKAMP, DR. G. WENZ, PROF. YUANZE XU, DR. K. YASE.

REFERENCES

1. H. Kuhn, D. Möbius, H. Bücher in: Physical Methods of Chemistry (A. Weissberger, B. Rossiter, eds.) Wiley, New York, 1972, vol. 1, p.577
2. D. Möbius, ed. Langmuir-Blodgett-Films-3, Thin Solid Films, 159, 1
3. H. Ringsdorf, B. Schlarb, J. Venzmer, Angew. Chem. Int. Ed. Engl. 27 (1988) 113
4. F. Embs, D. Funhoff, A. Laschewsky, U. Licht, H. Ohst, W. Prass, H. Ringsdorf, G. Wegner, R. Wehrmann, Adv. Mater. 3 (1991) 25
5. T. Arndt, G. Wegner in: Optical Techniques to Characterize Polymer Systems, H. Bässler, ed. Elsevier, London 1989, p. 41 f
6. G. Duda, A.J. Schouten, T. Arndt, G. Lieser, G.F. Schmidt, C. Bubeck, G. Wegner, Thin Solid Films, 159 (1988) 221
7. E. Orthmann, G. Wegner, Angew. Chem. Int. Ed. Engl. 25 (1986) 114

8. T. Sauer, T. Arndt, D.N. Batchelder, A.A. Kalachev, G. Wegner, Thin Solid Films 187 (1990) 357
9. T. Sauer, G. Wegner, Macromolecules 24 (1991) 2240
10. G. Duda, G. Wegner, Makromol. Chem. Rapid Commun. 9 (1988) 495
11. W. Hickel, G. Duda, M. Jurich, T. Kröhl, K. Rockford, G.I. Stegeman, J.D.Swalen, G. Wegner, W. Knoll, Langmuir 6 (1990) 1403
12. A. Ritcey, G. Wegner, G. Wenz, Makromol. Chem., in press
13. F.W. Embs, G, Wegner, D. Neher, P. Albouy, R.D. Miller, C.G. Willson, W. Schrepp, Macromolecules 24 (1991) 5068
14. S. Lee, I.R. Dutcher, B. Hillebrands, G.I. Stegeman, W. Knoll, G. Duda, G. Wegner, Mat. Res. Soc. Symp. Proc. 188 (1990) 355
15. F. Nizzoli, B. Hillebrands, S. Lee, G.I. Stegeman, G. Duda, G. Wegner, W. Knoll, Materials Sci. Eng. B5 (1990) 173
16. W. Hickel, G. Duda, G. Wegner, W. Knoll, Makromol. Chem. Rapid Commun. 10 (1989) 353
17. G. Wegner, K. Mathauer, Mat. Res. Soc. Symp. 247 (1992) 767
18. M. Schaub, K. Mathauer, S. Schwiegk, P.A. Albouy, G. Wenz, G. Wegner, Thin Solid Films , 210/211 (1992) 397
19. M. Seuffert, Diplomarbeit, Universität Mainz, Mainz 1992
20. T. Vahlenkamp, G. Wegner, to be published
21. W. Knoll, Mat. Res. Soc. Bull. XVI(7) (1991) 29
22. S. Schwiegk, H. Fischer, Y. Xu, F. Kremer and G. Wegner, Makromol. Chem., Macromol. Symp. 46 (1991) 211
23. S. Schwiegk, T. Vahlenkamp, Y. Xu, G. Wegner, Macromolecules 25 (1992) 25/3
24. W. Caseri, T. Sauer, G. Wegner, Makromol. Chem. Rapid Commun. 9 (1988) 651
25. T. Sauer, W. Caseri, G. Wegner, Mol. Cryst. Liq. Cryst. 183 (1990) 387
26. T. Sauer, W. Caseri, G. Wegner, A. Vogel, B. Hoffmann, J. Phys. D. Appl. Phys. 23 (1990) 79
27. M. Kasha, H.R. Rawls, M. Ashraf ElBayonni, Pure Appl. Chem., 11 (1965) 371
28. E.G. Rae, M. Kasha, In: L. Augenstein, R. Mason, B. Rosenberg (eds.) Physical Processes in Radiation Biology, Academic Press, New York, 1964
29. C. Bubeck, A. Grund, A. Kaltbeitzel, D. Neher, A. Mathy, G. Wegner, in J. Messier., Ed. "Organic Molecules for Nonlinear Optics and Photonics, Kluwer Publ. Dordrecht (1991) 398
30. S. Schwiegk, Ph. D. Thesis, University of Mainz, Mainz, Germany 1992
31. Ch. Bubeck, D. Holtkamp, Adv. Mater. 3 (1991) 32
32. S. Mittler-Neher, D. Neher, G.I. Stegemann, F.W. Embs, G. Wegner, Chem. Phys., 161 (1992) 289
33. K. Yase, S. Schwiegk, G. Lieser, G. Wegner, Thin Solid Films 213 (1992) 130
34. K. Yase, S. Schwiegk, G. Lieser, G. Wegner, Thin Solid Films 210/211 (1992) 22
35. B.R. Malcolm, Proc. R. Soc., London, Ser. A 305 (1968) 363

36. R. Loeb, R.E. Baier, J. Colloid Interface Sci. 27 (1968) 38
37. Takeda, M. Matsumoto, T. Takenaga, Z. Fujiyosji, N. Uyeda, J. Colloid Interface Sci. 91 (1983) 267
38. M. Foster, T.R. Vierheller, A. Schmidt, K. Mathauer, W. Knoll, G. Wegner, S. Satija, Ch. Majkrzak, Mat. Res. Soc. Symp. Proc., (1992), in press
39. K.H. Drexhage, M.M. Zwick, H. Kuhn, Ber. Bunsenges. Phys. Chem. 67 (1963) 62
40. Th. Förster, Z. Naturforsch. 4A (1949) 321
41. S. Ohomori, S. Ho, M. Yamamoto, Macromolecules 24 (1991) 2377
42. I. Berlman, Energy Transfer Parameters of Aromatic Compounds, Academic Press, New York, USA, 1973
43. K. Mathauer, G. Wegner, Macromolecules, in press
44. M. Schaub, Diplomarbeit, Universität Mainz, Mainz 1991
45. H.W. Spiess, Adv. Polym. Sci. 66 (1985) 23
46. I. Leisen, M. Werth, C. Boeffel, H.W. Spiess, J. Chem. Phys. (1992) in press
47. M. Werth, K. Schmidt-Rohr, H.W. Spiess, S. Schwiegk, G. Wegner, to be published
48. H.W. Spiess, H. Sillescu, J. Magn. Resonance 42 (1980) 381
49. M. Iida, M. Schulze, G. Wegner, unpublished
50. M. Seuffert, Diplomarbeit, Universität Mainz, 1991
51. K. Mathauer, A. Mathy, C. Bubeck, G. Wegner, W. Hickel, U. Scheunemann, Thin Solid Films 210/211 (1992) 449
52. J.G. Gaudiello, G.E. Kellog, S.M. Tetrick, H.O. Marcy, W.I. McCarthy, I.C. Butler, C.R. Kannewurf, T.J. Marks, J. Amer. Chem. Soc. 111 (1989) 5259, 5271
53. E.A. Orthmann, V. Enkelmann, G. Wegner, Makromol. Chem. Rapid Commun. 4 (1983) 687
54. A. Ferencz, N.R. Armstrong, G. Wegner, Langmuir, to be published
55. E.M. Genies, I.M. Pernaut, Synthetic Metals, 10 (1989) 117
56. B. Mann, H. Kuhn, J. Appl. Phys. 42 (1971) 4398
57. H. Fischer, B. Movaghar, G. Wegner, to be published
58. A. Vogel, B. Hoffmann, S. Schwiegk, G. Wegner, Sensors and Actuators, B4 (1991) 65, 379
59. R. Erbach, B. Hoffmann, M. Schaub, G. Wegner, Sensors and Actuators (1992), in press
60. A. Vogel, "Ionenselektive Feldeffektstrukturen mit Langmuir-Blodgett-Filmen" VDI-Fortschrittberichte, Reihe 8. Nr. 239 VDI-Velag, Düsseldorf 1991
61. P. Bergeveld, IEEE Trans. Biomed. Engl., 17 (1970) 70